

Article

The Influence of a High-Voltage Discharge in a Helicoidal Twisted-Pair Structure on Enzyme Adsorption

Yuri D. Ivanov ^{1,2,*}, Vadim Yu. Tatur ³, Ivan D. Shumov ¹ , Andrey F. Kozlov ¹, Anastasia A. Valueva ¹, Irina A. Ivanova ¹, Maria O. Ershova ¹, Nina D. Ivanova ^{3,4}, Igor N. Stepanov ³, Andrei A. Lukyanitsa ^{3,5} and Vadim S. Ziborov ^{1,2}

¹ Institute of Biomedical Chemistry, Pogodinskaya Str., 10 Build. 8, 119121 Moscow, Russia

² Joint Institute for High Temperatures of the Russian Academy of Sciences, 125412 Moscow, Russia

³ Foundation of Perspective Technologies and Novations, 115682 Moscow, Russia

⁴ Moscow State Academy of Veterinary Medicine and Biotechnology Named after Skryabin, 109472 Moscow, Russia

⁵ Faculty of Computational Mathematics and Cybernetics, Moscow State University, 119991 Moscow, Russia

* Correspondence: yurii.ivanov.nata@gmail.com

Abstract: The effect of a high-voltage discharge in a helicoidal structure on the adsorption properties of an enzyme on mica has been studied with the example of horseradish peroxidase (HRP). The discharge was generated at the expense of a sparkover in a 3 mm gap between two electrodes, to which a 10 kV, 50 Hz AC voltage was applied. The electrodes were connected to a twisted pair, which was wound onto a cone, forming the helicoidal structure. The incubation of the enzyme solution near the top of the helicoidal structure has been found to cause an increase in the degree of aggregation of HRP adsorbed on mica in comparison with the control HRP sample. The results obtained should be taken into account in studies of enzymes using biosensors with helicoidal structures as heating elements, as well as in refining models describing effects of low-frequency alternating current, flowing through helicoidal structures, on proteins and biological objects.

Keywords: atomic force microscopy; helicoidal structure; electric discharge; electromagnetic field; protein aggregation; enzyme adsorption



Citation: Ivanov, Y.D.; Tatur, V.Y.; Shumov, I.D.; Kozlov, A.F.; Valueva, A.A.; Ivanova, I.A.; Ershova, M.O.; Ivanova, N.D.; Stepanov, I.N.; Lukyanitsa, A.A.; et al. The Influence of a High-Voltage Discharge in a Helicoidal Twisted-Pair Structure on Enzyme Adsorption. *Electronics* **2022**, *11*, 3276. <https://doi.org/10.3390/electronics11203276>

Academic Editor: Jikui Luo

Received: 14 September 2022

Accepted: 10 October 2022

Published: 12 October 2022

Publisher's Note: MDPI stays neutral with regard to jurisdictional claims in published maps and institutional affiliations.



Copyright: © 2022 by the authors. Licensee MDPI, Basel, Switzerland. This article is an open access article distributed under the terms and conditions of the Creative Commons Attribution (CC BY) license (<https://creativecommons.org/licenses/by/4.0/>).

1. Introduction

Recently, the study of protein aggregation has attracted great interest owing to the involvement of protein aggregates in maintaining optimal body functioning. Such diseases as Alzheimer's [1–3], Parkinson's [1], cardiovascular [4], and oncological ones [5] are known to be associated with increased aggregation of proteins. A positive example of controlled protein aggregation is the dimerization of myeloperoxidase, which provides normal functioning of the body [6]. Certain amyloid proteins—for instance, FXR1 protein—are also necessary for optimal brain functioning [1].

Electromagnetic fields are known to have a significant impact on the human body, causing various pathologies [7–10]. Technological development leads to a steady increase in the level of electromagnetic background induced by power lines operated at 50 Hz industrial frequency. Such electromagnetic fields can affect the body, influencing blood rheology [11] or blood pressure [12]. When high-voltage lines are grounded, or when lightning strikes an electrical power line, significant electromagnetic fields are induced. Therefore, studying the effect of discharges from high-voltage sources, connected to various current-carrying structures, on biological objects is an important task. The circuits containing twisted-pair wires are the most interesting ones from the viewpoint of the organization of current-carrying signals and power circuits. The twisted pair represents a pair of conductors twisted together [13] in order to suppress losses in the transmission of electrical signals. Although the twisted pair is designed to provide suppression of losses, it normally emits

electromagnetic waves. It is known that even weak alternating electromagnetic fields of non-thermal power can change the properties of enzymes [14]. As regards alternating electromagnetic fields of low frequency, their action on enzymes can lead to either an increase or a decrease in the enzymatic activity, depending on the enzyme and the field parameters. Several membrane-associated enzymes (namely, alkaline phosphatase, acetylcholinesterase from blood cell membranes, acetylcholinesterase from synaptosomes, phosphoglycerate kinase, and adenylate kinase) were reported to lose their activity under the influence of a 75 Hz electromagnetic field, while other enzymes (CaATPase, Na/K ATPase, and succinic dehydrogenase) were found to be virtually insensitive to fields of this frequency [15]. A 20 Hz electromagnetic field was found to have a very significant stimulating effect on cAMP-dependent protein kinase [16]. As regards horseradish peroxidase (HRP) enzyme, its catalytic efficiency decreased nearly twofold after its exposure to a 50 Hz electromagnetic field, while being unaffected by a 100 Hz field [17].

Considering the impact of radiofrequency electromagnetic fields, radiofrequency heating (27.12 MHz 6 kW) was reported to have quite the opposite effect on the enzymatic activity of HRP [18]. While the treatment at 50 °C slightly increased the enzymatic activity, it significantly decreased after the heating at higher (70 °C and 90 °C) temperatures [18]. The exposure of HRP to either a 13.56 MHz, 915 MHz, or 2.45 GHz electromagnetic field was reported to have no nonthermal effect on HRP [19]. On the contrary, microwave treatment was reported to cause very significant inactivation of HRP [20], red beet peroxidase, and polyphenoloxidase [21].

In this work, the influence of a high-voltage discharge in a helicoidal structure, based on a twisted pair, on the properties of enzymes has been studied. As a helicoidal element, a twisted pair, wound onto a conical surface, has been employed. The discharge current flowed through a helicoidal structure of copper twisted pair wires during a discharge in the air gap between the electrodes from a high-voltage AC power supply (10 kV, 50 Hz). Similar discharge devices are used in voltage limiters [22]. As a model object, HRP has been used, since it is comprehensively characterized in the literature. It is known that HRP exists in solution in the form of monomers and aggregates [23,24]. Atomic force microscopy (AFM) has been employed to study the influence of a high-voltage discharge on the enzyme. AFM allows one to study the influence of electromagnetic fields on enzyme aggregation at the level of single molecules [14,23,25,26], revealing even subtle effects [26], when the electromagnetic field intensity is at the background level [23,26].

Our AFM study has revealed that the incubation of HRP solution near the top of a helicoidal structure upon flowing of a discharge current through this structure leads to an increased aggregation of the enzyme on a mica surface.

The results of our study can be used in the development of biosensors employing helicoidal conductive structures operating at industrial AC frequency, and for designing and refining models of the influence of alternating electromagnetic fields of various configurations on biological objects.

2. Materials and Methods

2.1. Chemicals and Enzyme

Horseradish peroxidase enzyme and its substrate 2,2'-azino-bis(3-ethylbenzothiazoline-6-sulfonate) (ABTS) were purchased from Sigma (enzyme: Cat. #6782). Disodium hydrogen orthophosphate, citric acid, and hydrogen peroxide (all of analytical or higher grade) were purchased from Reakhim (Moscow, Russia). Deionized (18.2 M Ω × cm) ultrapure water was obtained using a Simplicity UV system (Millipore, Molsheim, France).

2.2. Experimental Setup

Figure 1 displays a schematic of the experimental setup.

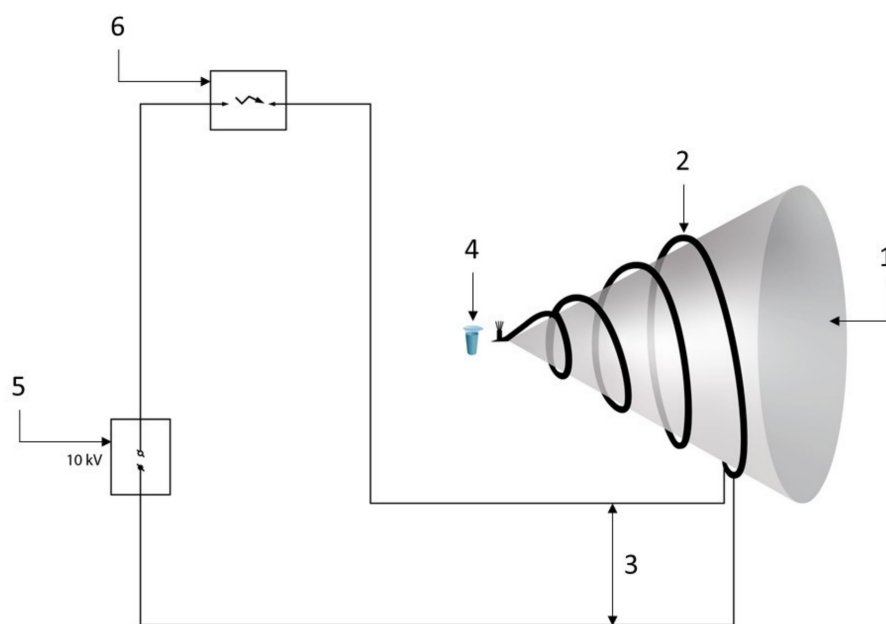


Figure 1. Experimental setup. Numbers indicate the main elements of the setup: the cone (1), the twisted pair helix (2), the soldered ends of the twisted pair wires (3), the test tube with the enzyme solution near the cone top (4), the high-voltage AC power supply (50 Hz frequency, 10 kV amplitude) unit (5), and the spark gap (6).

A cellulose cone with a base diameter of 210 mm and a 62° angle at the top was used as a conical structure. A twisted pair, fabricated from copper wires with a diameter of 1 mm in a polyvinyl chloride (PVC) sheath, was wound onto the cone, forming a helicoidal structure. The number of twists in the twisted pair was 70 per 1 m of length. The helicoidal structure was in the form of a densely packed (turn to turn) twisted pair. In this pair, from the side of the cone top, the copper wires were soldered, forming a continuation (3) of the top of the cone (see Figure 1), and from the side of the cone base, two copper wires of the twisted pair were brought out to the discharge gap (5). When a 50 Hz sinusoidal voltage from the voltage source (6) was applied to the discharge gap and reached the breakdown voltage of ~ 10 kV, a high-voltage discharge occurred, and the discharge current began to flow through the conductive helicoidal structure. This process was carried out for 10 min. Test tubes with HRP solution (10^{-7} M HRP in 2 mM Dulbecco's modified phosphate buffered saline, pH 7.4) were placed at a 2 cm distance from the top of the cone. The control HRP solution was placed in the same position, but with the power supply unit turned off. The exposure time of the protein solution in both the working (with the power supply unit turned on) and control (with the power supply unit turned off) experiments was ten minutes. After the exposure of the HRP to the helicoidal structure, mica AFM substrates were incubated in them. The mica substrates were subsequently studied by AFM as described below.

2.3. AFM Experiments

AFM experiments were performed using direct surface adsorption [27] of HRP onto mica using the well-established technique reported previously [14,25,28–31]. HRP was adsorbed onto freshly cleaved mica substrate from 800 μ L of 10^{-7} M HRP solution in 2 mM Dulbecco's modified phosphate buffered saline (pH 7.4) for 10 min at room temperature in a shaker at 600 rpm. After that, each substrate was rinsed with ultrapure water and dried. AFM measurements were carried out in the tapping mode in air with a Titanium multimode atomic force microscope (which pertains to the equipment of "Human Proteome" Core Facility of the Institute of Biomedical Chemistry, supported by the Ministry of Education and Science of the Russian Federation, agreement 14.621.21.0017, unique project IDRMEFI62117X0017; NT-MDT, Zelenograd, Russia) equipped with NSG10 cantilevers

("TipsNano", Zelenograd, Russia). The number of AFM scans obtained for each sample was no less than ten. Relative distributions of the imaged objects with height $\rho(h)$ were calculated as reported elsewhere [32]. In blank experiments with the use of protein-free buffer instead of HRP solution, no objects with heights over 0.5 nm were registered.

2.4. Spectrophotometry

Enzymatic activity of HRP was estimated by spectrophotometry using ABTS as substrate as reported in our previous papers [14,25,28–31] according to the technique reported by Sanders et al. [33].

3. Results

Our experiments were carried out in an experimental setup, in which high-voltage discharges with a 50 Hz frequency were generated. The discharge current flowed through a helicoidal structure wound onto a cone. Figure 2 displays a typical AFM image of mica substrate incubated in HRP enzyme solution after its exposure near the top of the cone upon flowing of the discharge current through the twisted pair winding. For comparison, a typical AFM image of substrate incubated in the control HRP sample, which was located in the same place with the AC power supply turned off, is also presented. Right panels display the respective cross-section profiles marked with lines in the AFM images.

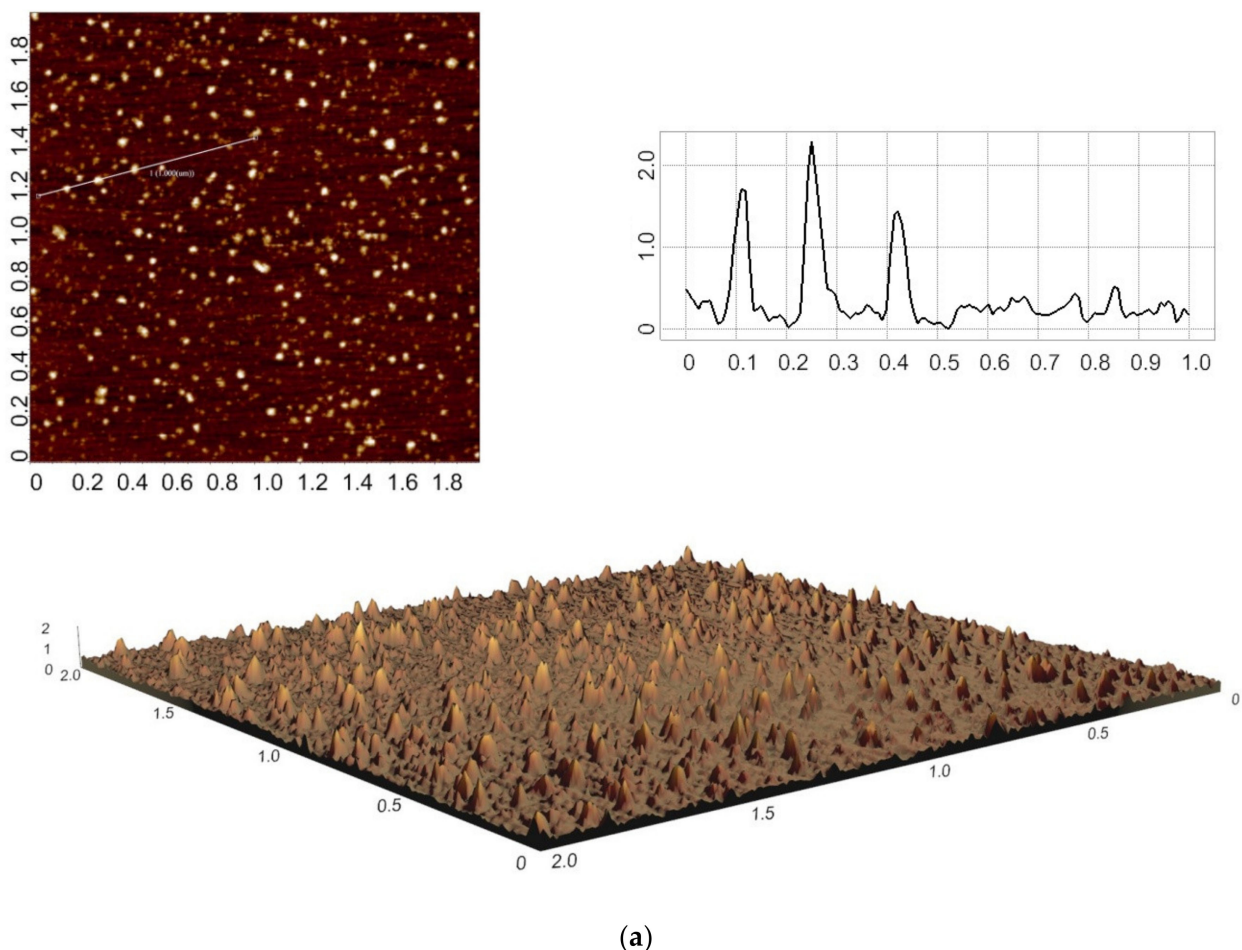


Figure 2. Cont.

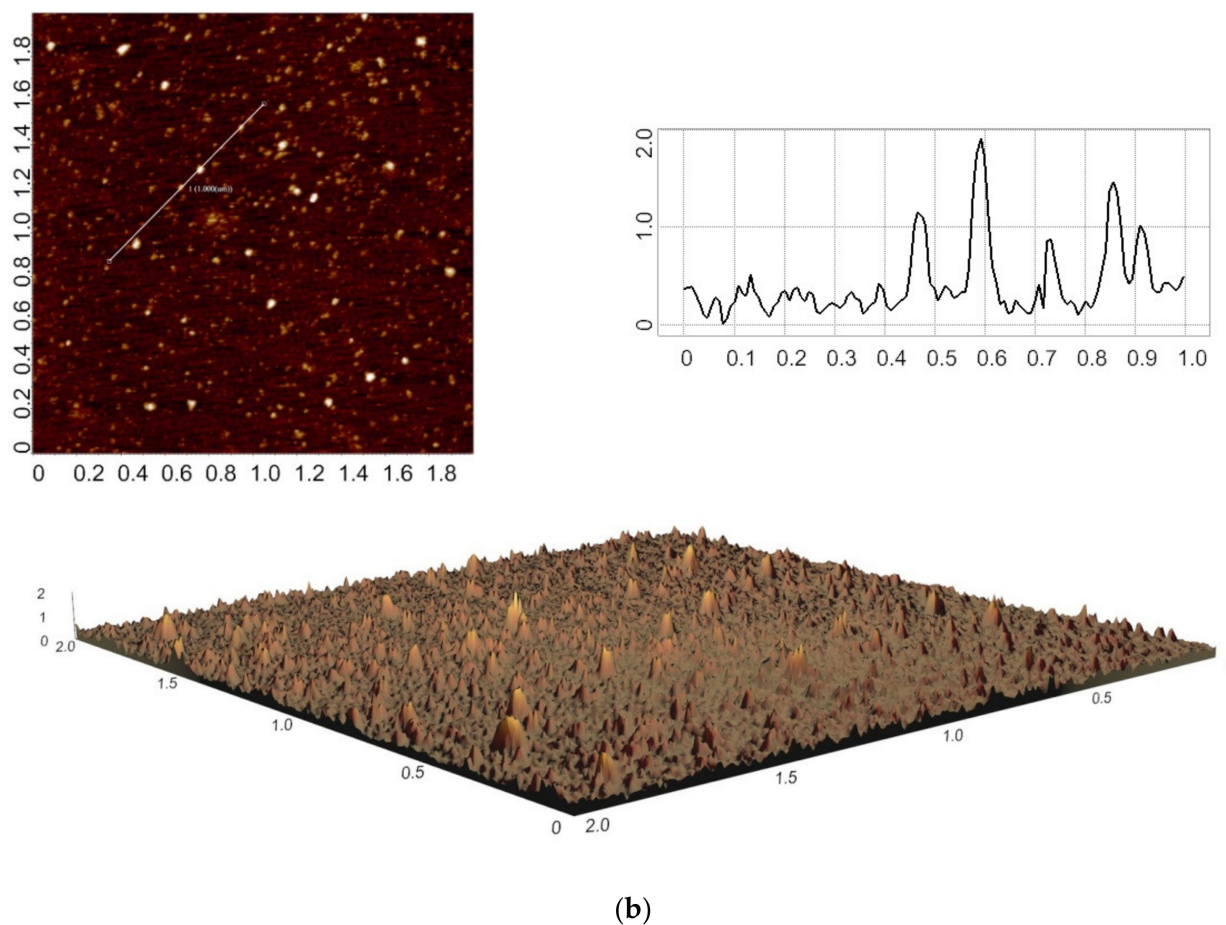


Figure 2. Typical 2D (top left) and 3D (bottom) AFM images (scan size $2 \times 2 \mu\text{m}$, Z scale 2 nm) and corresponding cross-section profiles (top right; X scale $1 \mu\text{m}$; Y scale 2 nm) of mica substrates incubated in HRP solutions, which exposed near the top of the cone with the AC power supply turned on (a) and off ((b), control experiment). Experimental conditions: the solution contained 10^{-7} M HRP in 2 mM Dulbecco's modified phosphate buffered saline (pH 7.4); 10 kV, 50 Hz sinusoidal voltage was applied from the power supply (a).

As can be seen from Figure 2, under experimental conditions with high voltage applied from the power supply, objects with heights exceeding 0.5 nm were observed on the mica substrate surface after its incubation in the HRP solution. In control experiments performed in the absence of electric current through the helicoidal structure, objects with such heights were also observed. It should be noted that in blank experiments with protein-free buffer, no objects with heights exceeding 0.5 nm were observed. Accordingly, for these considerations, objects with >0.5 nm heights were attributed to HRP biomolecules.

Next, the relative and absolute distributions of AFM images of objects with heights were plotted. Figure 3 displays relative height distributions $\rho(h)$ of the objects visualized in the working and control experiments.

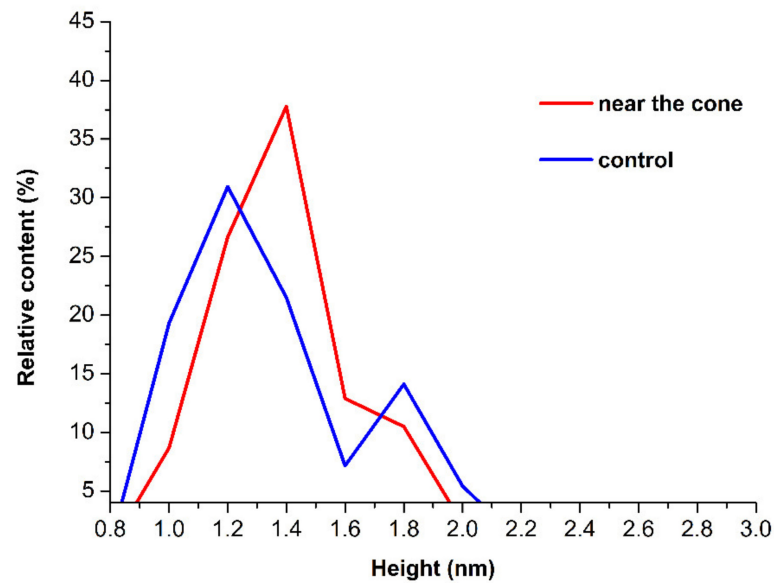


Figure 3. Relative height distributions of objects visualized by AFM on mica substrates incubated near the top of the cone with the power supply turned on (red curve) or off (blue curve).

As one can see in Figure 3, the majority of particles, visualized in the case of the control sample, had a height of 1.2 nm. Another maximum for the control sample corresponded to 1.8 nm height. In contrast, for the sample incubated in the working experiment, the first maximum corresponded to 1.4 nm height, and the second maximum corresponded to the height range from 1.6 to 1.8 nm. Accordingly, for HRP incubated near the top of the cone in the working experiment with the voltage applied (when current flowed through its winding), a shift towards an increase in the relative number of objects with 1.4–1.6 nm heights in the right wing of the distribution was observed—in comparison with the distribution obtained in the absence of current through the winding of the cone.

Figure 4 displays a histogram of absolute height distributions of the objects visualized in the working and control experiments.

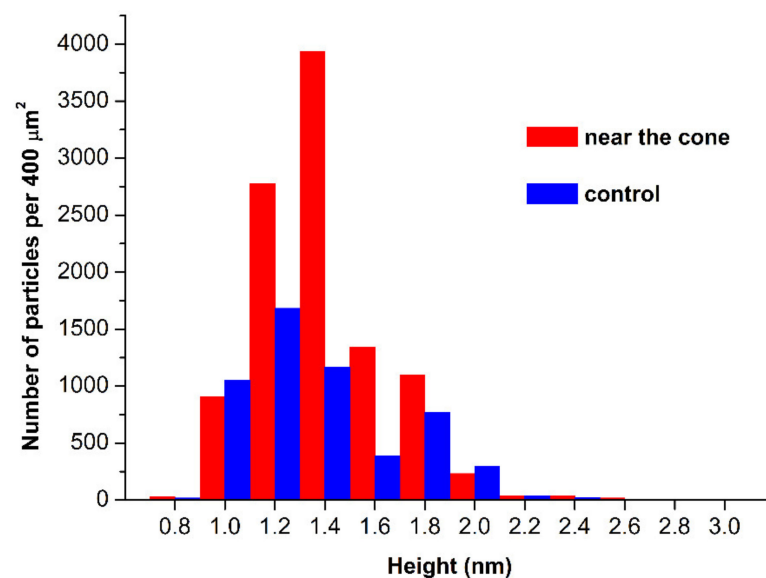


Figure 4. Absolute height distributions of objects visualized by AFM on mica substrates incubated near the top of the cone with the power supply turned on (red bars) or off (blue bars). The absolute distribution indicates the number of particles normalized to a scanned area of 400 μm². The experimental error was ±250 particles per 400 μm².

For HRP incubated near the top of the cone with the voltage applied (when current flowed through its winding), a shift towards an increase in the relative number of objects with 1.4–1.6 nm heights was observed in the absolute height distribution—in comparison with the distribution obtained in the absence of current through the winding of the cone. Namely, an increase in the proportion of HRP particles with greater heights was observed in the case of voltage applied, as compared to the case without the application of the voltage to the cone winding. As regards the absolute distributions of adsorbed objects with heights, approximately the same number of adsorbed objects was observed in both the control and working experiments.

Spectrophotometry measurements revealed no change in the enzymatic activity of HRP after its exposure to the high-voltage discharge in a helicoidal twisted-pair structure.

4. Discussion

In this work, the effect of a high-voltage discharge generated with an AC power supply (50 Hz) in a helicoidal structure, formed by a twisted pair wound onto a cone, on an enzyme was studied using HRP as a model object. For this purpose, comparative measurements of the adsorption properties of HRP on mica substrates were carried out. In the working experiments, the substrates were incubated in HRP solution exposed near the top of the helicoidal structure with an alternating current flowing through the winding of the cone. In contrast, in the control experiments, the power supply was turned off. The height distributions of objects adsorbed from these enzyme solutions, under respective experimental conditions, were then plotted.

For the HRP solution exposed to the high-voltage discharge, an increase in the aggregation of HRP on mica was observed, as the relative content of 1.4–1.6 nm objects increased.

This conclusion about the increase in aggregation during the flow of alternating current is drawn based on the fact that, according to the literature [23], horseradish peroxidase adsorbs from its solution onto mica AFM substrates as a mixture of monomers and aggregates. For monomers, the maximum of the relative height distribution is 1.2 nm [14], while aggregates typically have greater heights (~1.4 nm for lower-order aggregates, and ~1.8 nm for higher-order ones), and this is what we observed in our AFM experiments reported herein. Accordingly, the greater the ratio between objects with a height of ≥ 1.4 nm in relation to the number of objects with a height of 1–1.2 nm, the higher the degree of HRP aggregation.

Such changes in the protein are probably associated with a change in the surface structure of the protein shell, which leads to changes in the adsorption properties on the mica surface. The nature of these changes can be as follows. When current flows through a twisted pair, electromagnetic radiation can occur. It is known that weak alternating magnetic fields can cause significant changes in the structure of water [34]. These changes, in turn, can alter the ratio between para- and ortho-isomers of water [35] and, accordingly, affect the hydration shell of the enzyme biomolecules. The presence of the hydration shell around a biomolecule is an essential factor, since it influences the biomolecule's structure [36,37] and functionality [38–40]. As regards enzyme biomolecules, enzymatic activity was reported to be influenced by the hydration shell [38–40]. Upon adsorption onto a solid substrate, the aggregation of the enzyme is determined by the interaction of its molecules with each other, with the solvent [25], and with the substrate surface. These interactions can well be affected by changes in the hydration shell of the enzyme biomolecules. This explains the change in the aggregation of the enzyme on the surface of the mica substrates.

In general, the effect of an electric field on enzymes can be different depending on the experimental conditions. Namely, Poojary et al. reported that many enzymes are inactivated by the action of a pulsed electric field [41]. As regards the HRP enzyme, Zhong et al. reported its inactivation by a 5 to 25 kV/cm pulsed electric field, which affected the secondary structure of the enzyme [42,43]. Nevertheless, Ohshima et al. [44] demonstrated a stimulating effect of a pulsed electric field on the activity of horseradish peroxidase at

short (~50 s) treatment times and moderate (≤ 12 kV/cm) electric field strength, while longer treatment and/or stronger electric field induced enzyme inactivation [44]. In our experiments, a 10 kV electric discharge had no effect on the HRP enzymatic activity.

As regards the effect of electric field treatment on protein aggregation, in their recent review, Vanga et al. reported that pulsed electric field treatment induced aggregation of a number of proteins and enzymes [45], and this is what we observed for HRP on mica after the enzyme exposition to an electric discharge.

The results obtained in our experiments should be taken into account in further investigation of the effect of conductive conical elements, containing helicoidal structures with alternating voltage, on biological objects. This can be of use in the development of biosensors and bioreactors, in which spiral (i.e., helicoidal) structures can be used as heating elements [46–48]. Our results can also find their application in the development of other electrodynamic systems employing helicoidal structures, e.g., heart valves, where helicoidal structures are used to reduce valve fouling when the current of charged blood particles flows. The results obtained are of interest when modeling the effects of electromagnetic fields induced by electric discharges and twisted pairs, on enzyme systems, and on the human body. Our results can also be useful for studying the processes occurring in twisted pairs, which have a converging in space helicoidal structure, which can be used in the generation of spatially directed electromagnetic fields.

5. Conclusions

The effect of a high-voltage discharge, generated with a 10 kV, 50 Hz AC voltage applied to a twisted-pair helicoidal structure wound onto a cone, on the physicochemical properties of HRP has been demonstrated. An increase in the degree of aggregation of HRP molecules adsorbed on mica from the enzyme solution, exposed near the top of the helicoidal structure, has been observed in comparison with the enzyme solution exposed in the absence of applied voltage. The results obtained can find their application in designing various elements used in current-carrying systems based on twisted pairs, as well as other conductive helicoidal structures, and in modeling processes in environments containing conical valves and in other applications—for instance, as 3D helicoidal heating elements in biosensors and bioreactors.

Author Contributions: Conceptualization, Y.D.I. and V.S.Z.; Data curation, A.A.V. and M.O.E.; Formal analysis, N.D.I., V.Y.T. and V.S.Z.; Investigation, Y.D.I., A.F.K., I.D.S., A.A.V., I.A.I., M.O.E., I.N.S. and V.S.Z.; Methodology, Y.D.I. and V.S.Z.; Project administration, Y.D.I.; Resources, V.Y.T., I.N.S., A.A.L. and V.S.Z.; Software, A.A.L. and V.S.Z.; Supervision, Y.D.I.; Validation, V.S.Z.; Visualization, I.D.S. and A.A.V.; Writing—original draft, Y.D.I. and I.D.S.; Writing—review and editing, Y.D.I. All authors have read and agreed to the published version of the manuscript.

Funding: This work was financed by the Ministry of Science and Higher Education of the Russian Federation within the framework of state support for the creation and development of World-Class Research Centers “Digital Biodesign and Personalized Healthcare” No. 075-15-2022-305.

Data Availability Statement: Correspondence and requests for materials should be addressed to Y.D.I.

Acknowledgments: The AFM measurements were performed employing a titanium multimode atomic force microscope, which pertains to “Avogadro” large-scale research facilities.

Conflicts of Interest: The authors declare no conflict of interest.

References

1. Sopova, J.V.; Koshel, E.I.; Belashova, T.A.; Zadorsky, S.P.; Sergeeva, A.V.; Siniukova, V.A.; Shenfeld, A.A.; Velizhanina, M.E.; Volkov, K.V.; Nizhnikov, A.A.; et al. RNA-binding protein FXR1 is presented in rat brain in amyloid form. *Sci. Rep.* **2019**, *9*, 18983. [CrossRef] [PubMed]
2. Benseny-Cases, N.; Álvarez-Marimon, E.; Aso, E.; Carmona, M.; Klementieva, O.; Appelhans, D.; Ferrer, I.; Cladera, J. In situ structural characterization of early amyloid aggregates in Alzheimer's disease transgenic mice and *Octodon degus*. *Sci. Rep.* **2020**, *10*, 5888. [CrossRef] [PubMed]
3. Zhang, X.; Fu, Z.; Meng, L.; He, M.; Zhang, Z. The early events that initiate β -amyloid aggregation in Alzheimer's disease. *Front. Aging Neurosci.* **2018**, *10*, 359. [CrossRef] [PubMed]
4. Gouveia, M.; Xia, K.; Colón, W.; Vieira, S.I.; Ribeiro, F. Protein aggregation, cardiovascular diseases, and exercise training: Where do we stand? *Ageing Res. Rev.* **2017**, *40*, 1–10. [CrossRef]
5. Xu, J.; Reumers, J.; Couceiro, J.R.; De Smet, F.; Gallardo, R.; Rudyak, S.; Cornelis, A.; Rozenski, J.; Zwolinska, A.; Marine, J.C.; et al. Gain of function of mutant p53 by coaggregation with multiple tumor suppressors. *Nat. Chem. Biol.* **2011**, *7*, 285–295. [CrossRef]
6. Gavrilenko, T.I.; Ryzhkova, N.A.; Parkhomenko, A.N. Myeloperoxidase and its role in development of ischemic heart disease. *Ukr. J. Cardiol.* **2014**, *4*, 119–126.
7. Ahibom, A.; Day, N.; Feychting, M.; Roman, E.; Skinner, J.; Dockerty, J.; Linet, M.; McBride, M.; Michaelis, J.; Olsen, J.H.; et al. A pooled analysis of magnetic fields and childhood leukaemia. *Br. J. Cancer* **2000**, *83*, 692–698. [CrossRef]
8. Dowson, D.I.; Lewith, G.T.; Campbell, M.; Mullee, M.A.; Brewster, L.A. Overhead high-voltage cables and recurrent headache and depressions. *Practitioner* **1988**, *232*, 435–436.
9. Greenland, S.; Sheppard, A.R.; Kaune, W.T.; Poole, C.; Kelsh, M.A. A pooled analysis of magnetic fields, wire codes, and childhood leukemia. *Epidemiology* **2000**, *11*, 624–634. Available online: <http://www.jstor.org/stable/3703814> (accessed on 14 September 2022). [CrossRef]
10. Perry, S.; Pearl, L.; Binns, R. Power frequency magnetic field; depressive illness and myocardial infarction. *Public Health* **1989**, *103*, 177–180. [CrossRef]
11. El-Kaliuoby, M.I.; El-Khatib, A.; Mohamed, M.; Roston, G.; Khalil, A.M.; Ahmed, M.M.; AbdulSalam, H. Monitoring of Rat's Blood Rheology after Exposure to 50-Hz Electric Fields (Occupational Study). *OSR J. Environ. Sci. Toxicol. Food Technol.* **2016**, *10*, 4–8. [CrossRef]
12. Korpinen, L.; Partanen, J. Influence of 50-Hz electric and magnetic fields on human blood pressure. *Radiat. Environ. Biophys.* **1996**, *35*, 199–204. [CrossRef]
13. Mahfouz, A.; Hassan, S.A.; Arisha, A. Practical simulation application: Evaluation of process control parameters in Twisted-Pair Cables manufacturing system. *Simul. Model. Pract. Theory* **2010**, *18*, 471–482. [CrossRef]
14. Ivanov, Y.D.; Pleshakova, T.O.; Shumov, I.D.; Kozlov, A.F.; Ivanova, I.A.; Valueva, A.A.; Tatur, V.Y.; Smelov, M.V.; Ivanova, N.D.; Ziborov, V.S. AFM imaging of protein aggregation in studying the impact of knotted electromagnetic field on a peroxidase. *Sci. Rep.* **2020**, *10*, 9022. [CrossRef]
15. Morelli, A.; Ravera, S.; Panfoli, I.; Pepe, I.M. Effects of extremely low frequency electromagnetic fields on membrane-associated enzymes. *Arch. Biochem. Biophys.* **2005**, *441*, 191–198. [CrossRef]
16. Thumm, S.; Löschinger, M.; Glock, S.; Hämmerle, H.; Rodemann, H.P. Induction of cAMP-dependent protein kinase A activity in human skin fibroblasts and rat osteoblasts by extremely low-frequency electromagnetic fields. *Radiat. Environ. Biophys.* **1999**, *38*, 195–199. [CrossRef]
17. Caliga, R.; Maniu, C.L.; Mihășan, M. ELF-EMF exposure decreases the peroxidase catalytic efficiency in vitro. *Open Life Sci.* **2016**, *11*, 71–77. [CrossRef]
18. Yao, Y.; Zhang, B.; Pang, H.; Wang, Y.; Fu, H.; Chen, X.; Wang, Y. The effect of radio frequency heating on the inactivation and structure of horseradish peroxidase. *Food Chem.* **2023**, *398*, 133875. [CrossRef]
19. Fortune, J.A.; Wu, B.-I.; Klivanov, A.M. Radio Frequency Radiation Causes No Nonthermal Damage in Enzymes and Living Cells. *Biotechnol. Prog.* **2010**, *26*, 1772–1776. [CrossRef]
20. Lopes, L.C.; Barreto, M.T.; Gonçalves, K.M.; Alvarez, H.M.; Heredia, M.F.; De Souza, R.O.M.; Cordeiro, Y.; Dariva, C.; Fricks, A.T. Stability and structural changes of horseradish peroxidase: Microwave versus conventional heating treatment. *Enzym. Microb. Technol.* **2015**, *69*, 10–18. [CrossRef]
21. Latorre, M.E.; Bonelli, P.R.; Rojas, A.M.; Gerschenson, L.N. Microwave inactivation of red beet (*Beta vulgaris* L. var. *conditiva*) peroxidase and polyphenoloxidase and the effect of radiation on vegetable tissue quality. *J. Food Eng.* **2012**, *109*, 676–684. [CrossRef]
22. Available online: <https://electricps.ru/razriad> (accessed on 14 September 2022).
23. Ivanov, Y.D.; Tatur, V.Y.; Pleshakova, T.O.; Shumov, I.D.; Kozlov, A.F.; Valueva, A.A.; Ivanova, I.A.; Ershova, M.O.; Ivanova, N.D.; Stepanov, I.N.; et al. The Effect of Incubation near an Inversely Oriented Square Pyramidal Structure on Adsorption Properties of Horseradish Peroxidase. *Appl. Sci.* **2022**, *12*, 4042. [CrossRef]
24. Ignatenko, O.V.; Sjölander, A.; Hushpulian, D.M.; Kazakov, S.V.; Ouporov, I.V.; Chubar, T.A.; Poloznikov, A.A.; Ruzgas, T.; Tishkov, V.I.; Gorton, L.; et al. Electrochemistry of chemically trapped dimeric and monomeric recombinant horseradish peroxidase. *Adv. Biosens. Bioelectron.* **2013**, *2*, 25–34.

25. Ziborov, V.S.; Pleshakova, T.O.; Shumov, I.D.; Kozlov, A.F.; Valueva, A.A.; Ivanova, I.A.; Ershova, M.O.; Larionov, D.I.; Evdokimov, A.N.; Tatur, V.Y.; et al. The Impact of Fast-Rise-Time Electromagnetic Field and Pressure on the Aggregation of Peroxidase upon Its Adsorption onto Mica. *Appl. Sci.* **2021**, *11*, 11677. [CrossRef]
26. Ivanov, Y.D.; Tatur, V.Y.; Pleshakova, T.O.; Shumov, I.D.; Kozlov, A.F.; Valueva, A.A.; Ivanova, I.A.; Ershova, M.O.; Ivanova, N.D.; Repnikov, V.V.; et al. Effect of Spherical Elements of Biosensors and Bioreactors on the Physicochemical Properties of a Peroxidase Protein. *Polymers* **2021**, *13*, 1601. [CrossRef] [PubMed]
27. Kiselyova, O.I.; Yaminsky, I.V.; Ivanov, Y.D.; Kanaeva, I.P.; Kuznetsov, V.Y.; Archakov, A.I. AFM study of membrane proteins, cytochrome P450 2B4, and NADPH-Cytochrome P450 reductase and their complex formation. *Arch. Biochem. Biophys.* **1999**, *371*, 1–7. [CrossRef] [PubMed]
28. Ivanov, Y.D.; Pleshakova, T.O.; Shumov, I.D.; Kozlov, A.F.; Ivanova, I.A.; Valueva, A.A.; Ershova, M.O.; Tatur, V.Y.; Stepanov, I.N.; Repnikov, V.V.; et al. AFM study of changes in properties of horseradish peroxidase after incubation of its solution near a pyramidal structure. *Sci. Rep.* **2021**, *11*, 1–9. [CrossRef]
29. Ivanov, Y.D.; Pleshakova, T.O.; Shumov, I.D.; Kozlov, A.F.; Romanova, T.S.; Valueva, A.A.; Tatur, V.Y.; Stepanov, I.N.; Ziborov, V.S. Investigation of the Influence of Liquid Motion in a Flow-based System on an Enzyme Aggregation State with an Atomic Force Microscopy Sensor: The Effect of Water Flow. *Appl. Sci.* **2020**, *10*, 4560. [CrossRef]
30. Ziborov, V.S.; Pleshakova, T.O.; Shumov, I.D.; Kozlov, A.F.; Ivanova, I.A.; Valueva, A.A.; Tatur, V.Y.; Negodailov, A.N.; Lukyanitsa, A.A.; Ivanov, Y.D. Investigation of the Influence of Liquid Motion in a Flow-Based System on an Enzyme Aggregation State with an Atomic Force Microscopy Sensor: The Effect of Glycerol Flow. *Appl. Sci.* **2020**, *10*, 4825. [CrossRef]
31. Ivanov, Y.D.; Pleshakova, T.O.; Shumov, I.D.; Kozlov, A.F.; Valueva, A.A.; Ivanova, I.A.; Ershova, M.O.; Larionov, D.I.; Repnikov, V.V.; Ivanova, N.D.; et al. AFM and FTIR Investigation of the Effect of Water Flow on Horseradish Peroxidase. *Molecules* **2021**, *26*, 306. [CrossRef]
32. Pleshakova, T.O.; Kaysheva, A.L.; Shumov, I.D.; Ziborov, V.S.; Bayzhanova, J.M.; Konev, V.A.; Uchaikin, V.F.; Archakov, A.I.; Ivanov, Y.D. Detection of hepatitis C virus core protein in serum using aptamer-functionalized AFM chips. *Micromachines* **2019**, *10*, 129. [CrossRef]
33. Sanders, S.A.; Bray, R.C.; Smith, A.T. pH-Dependent properties of a mutant horseradish peroxidase isoenzyme C in which Arg38 has been replaced with lysine. *Eur. J. Biochem.* **1994**, *224*, 1029–1037. [CrossRef]
34. Kiselyov, V.F.; Saletskii, A.M.; Semikhina, L.P. Structural changes in water after exposure to weak alternating magnetic fields. *Vestn. MSU. Series 3 Physics. Astron.* **1990**, *31*, 53–58.
35. Pershin, S.M. The Physical Basis of the Weak Fields Interaction with Bio Objects Is the Quantum Differences of H₂O Spin-Isomers. Online Biophysical Blog. Available online: <http://www.biophys.ru/archive/congress2012/proc-p27.htm> (accessed on 14 September 2022).
36. Pershin, S.M. Conversion of ortho-para H₂O isomers in water and a jump in erythrocyte fluidity through a microcapillary at a temperature of 36.6 ± 0.3 °C. *Phys. Wave Phenom.* **2009**, *17*, 241–250. [CrossRef]
37. Morón, M.C. Protein hydration shell formation: Dynamics of water in biological systems exhibiting nanoscopic cavities. *J. Mol. Liq.* **2021**, *337*, 116584. [CrossRef]
38. Fogarty, A.C.; Laage, D. Water Dynamics in Protein Hydration Shells: The Molecular Origins of the Dynamical Perturbation. *J. Phys. Chem. B* **2014**, *118*, 7715–7729. [CrossRef]
39. Verma, P.K.; Rakshit, S.; Mitra, R.K.; Pal, S.K. Role of hydration on the functionality of a proteolytic enzyme α -chymotrypsin under crowded environment. *Biochimie* **2011**, *93*, 1424–1433. [CrossRef]
40. Laage, D.; Elsaesser, T.; Hynes, J.T. Water Dynamics in the Hydration Shells of Biomolecules. *Chem. Rev.* **2017**, *117*, 10694–10725. [CrossRef]
41. Poojary, M.M.; Roohinejad, S.; Koubaa, M.; Barba, F.J.; Passamonti, P.; Jambrak, A.R.; Oey, I.; Greiner, R. Impact of Pulsed Electric Fields on Enzymes. In *Handbook of Electroporation*; Miklavčič, D., Ed.; Springer: Cham, Switzerland, 2017. [CrossRef]
42. Zhong, K.; Hu, X.; Zhao, G.; Chen, F.; Liao, X. Inactivation and conformational change of horseradish peroxidase induced by pulsed electric field. *Food Chem.* **2005**, *92*, 473–479. [CrossRef]
43. Zhong, K.; Wu, J.; Wang, Z.; Chen, F.; Liao, X.; Hu, X.; Zhang, Z. Inactivation kinetics and secondary structural change of PEF-treated POD and PPO. *Food Chem.* **2007**, *100*, 115–123. [CrossRef]
44. Ohshima, T.; Tamura, T.; Sato, M. Influence of pulsed electric field on various enzyme activities. *J. Electrostat.* **2007**, *65*, 156–161. [CrossRef]
45. Vanga, S.K.; Wang, J.; Jayaram, S.; Raghavan, V. Effects of Pulsed Electric Fields and Ultrasound Processing on Proteins and Enzymes: A Review. *Processes* **2021**, *9*, 722. [CrossRef]
46. Jeroish, Z.E.; Bhuvaneshwari, K.S.; Samsuri, F.; Narayanamurthy, V. Microheater: Material, design, fabrication, temperature control, and applications—A role in COVID-19. *Biomed Microdevices* **2022**, *24*, 3. [CrossRef] [PubMed]
47. Jung, W.; Lee, S.; Hwang, Y. Truly 3D microfluidic heating system with iterative structure of coil heaters and fluidic channels. *Smart Mater. Struct.* **2022**, *31*, 035016. [CrossRef]
48. Available online: <https://www.fermentador-bioreactor.com/en/features/precise-temperature-regulation-with-soft-ir-heating/> (accessed on 14 September 2022).